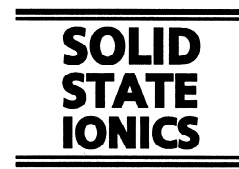




ELSEVIER

Solid State Ionics 97 (1997) 33–37



# Protons in $\text{LaMO}_3$ : atomistic modelling and ab initio studies

M.S. Islam\*, M. Cherry

*Department of Chemistry, University of Surrey, Guildford GU2 5XH, UK*

---

## Abstract

A combination of atomistic simulation and quantum mechanical techniques have been used to investigate proton transport phenomena in  $\text{LaMO}_3$  perovskite-structured oxides. We examine the energetics of dopant substitution and of incorporation of water to yield hydroxyl groups. The energy barrier to proton transfer between neighbouring oxygen ions is evaluated by ab initio cluster calculations. The simulation results suggest that a key step for proton migration is the relaxation energy required for the two adjacent oxygen ions to acquire equivalent lattice environments preceding proton transfer.

*Keywords:* Computer simulation; Proton transport; Perovskite oxide

*Materials:*  $\text{LaMnO}_3$

---

## 1. Introduction

Mixed metal oxides with the  $\text{ABO}_3$  perovskite structure have received considerable attention as high temperature proton conductors with potential applications in fuel cells, hydrogen sensors and steam electrolysis [1,2]. Most attention has focused on  $\text{A}^{2+}\text{B}^{4+}\text{O}_3$  perovskites, particularly  $\text{ACeO}_3$  ( $\text{A} = \text{Sr}, \text{Ba}$ ) [3–11] and  $\text{AZrO}_3$  ( $\text{A} = \text{Ca}, \text{Sr}$ ) [12–16] which contain acceptor dopants at the B sites compensated by oxygen vacancies. There have also been a few studies on proton conductivity in  $\text{A}^{3+}\text{B}^{3+}\text{O}_3$  type materials such as  $\text{LaYO}_3$  [17] and  $\text{LaErO}_3$  [18]. It is well known that the  $\text{LaMO}_3$  systems comprise a rich family of compounds that exhibit high oxygen ion conductivity and find use in solid oxide fuel cells

[19]. Recent developments have included complex perovskites of the types  $\text{A}_2\text{B}'\text{B}''\text{O}_6$  and  $\text{A}_3\text{B}'\text{B}''\text{O}_9$  (e.g.  $\text{Sr}_2\text{GaNbO}_6$  and  $\text{Sr}_3\text{CaNb}_2\text{O}_9$ ), in which oxygen vacancies are created by varying the  $\text{B}'/\text{B}''$  ratio [20]. When all of these perovskite oxides are exposed to water vapour at high temperatures, the oxygen vacancies are replaced by hydroxyl groups in which the interstitial proton is closely associated with an oxygen ion.

Improving our understanding of the underlying transport properties and the nature of the proton transfer mechanism has been the impetus behind a few recent investigations; this includes isotope effect ( $\text{D}_2\text{O}$  vs  $\text{H}_2\text{O}$ ) measurements [20,21] and quasi-elastic neutron scattering experiments [13]. We have already obtained via computer simulation techniques valuable microscopic information on the mechanistic features controlling oxygen ion transport in the  $\text{LaMO}_3$  perovskites (where  $\text{M} = \text{Cr}, \text{Mn}, \text{Fe}, \text{Co}$ ) [22,23]. This paper will amplify this knowledge by reviewing recent investigations of proton transport

---

\*Corresponding author. E-mail: m.islam@surrey.ac.uk; fax: +44-1483-259514

phenomena in  $\text{LaMO}_3$  using a combination of atomistic simulation and ab initio methods. These complementary computational tools are well suited to probing defect energetics and ion migration mechanisms in solid state ionic materials.

## 2. Computational methods

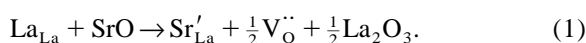
Since the simulation techniques have been described comprehensively elsewhere [24] only a brief overview is given here. The interatomic potentials are based on the Born model of the solid, which includes a long-range Coulombic interaction and a short-range term to model overlap-repulsions and van der Waals forces; the electronic polarisability of the ions is described by the shell model. In addition, the O–H interaction is modelled using an attractive Morse potential. The potential parameters were taken from our previous study of oxygen ion transport in  $\text{LaMO}_3$  [22] which successfully reproduce the observed perovskite structures. The defect energies were simulated using the Mott–Littleton approach [24] in which the ions in an inner region around the defect were relaxed explicitly, and ions in the surrounding crystal were treated using a continuum method.

The energy barrier to proton transfer has been investigated using ab initio Hartree–Fock techniques embodied in the CADPAC code [25]. An embedded cluster of 13 lattice ions is used with the surrounding crystal lattice represented by an array of point charges which reproduce the correct electrostatic potential. The calculations were based upon the  $\text{LaAlO}_3$  system, with high quality basis sets: Al 8–511G, O 8–411G, and H 6–311G. The Al and O basis sets were optimised for  $\text{Al}_2\text{O}_3$  and therefore particularly applicable to the present system; La is represented by the use of a model pseudopotential based upon Y. The calculations were performed at the SCF HF level with single point correlation effects included by the addition of Møller–Plesset perturbation theory to the second order (MP2). The calculations include polarisation functions for both the proton and oxygen ions and also allow full relaxation of the proton, the two neighbouring oxygen ions and the central Al ion.

## 3. Results and discussion

### 3.1. Incorporation of dopants and water

It has been shown that the incorporation of aliovalent dopants into the  $\text{LaMO}_3$  perovskites is crucial to the uptake of protons. These materials are typically ‘acceptor-doped’ with divalent ions (e.g.  $\text{Sr}^{2+}$ ) at the  $\text{La}^{3+}$  site, resulting in charge-compensating oxygen vacancies at low vapour pressures; this reaction can be represented in Kröger–Vink notation by the defect equation:



The energetics of this ‘solution’ reaction can be evaluated by our simulation approach in which we combine appropriate defect and lattice energy terms. The calculated solution energies for a series of alkaline-earth dopants in  $\text{LaMO}_3$  ( $M = \text{Mn, Fe, Co}$ ) are presented as a function of ion size in Fig. 1.

Examination of the results reveals that the most favourable energies and hence the highest solubilities are predicted for Sr and Ca in all the  $\text{LaMO}_3$  hosts. We also find a strong correlation between the calculated solution energy and the dopant size with minima near the ionic radius of  $\text{La}^{3+}$ . Solution of Sr and Ca will therefore enhance proton uptake owing to the increase in the concentration of oxygen

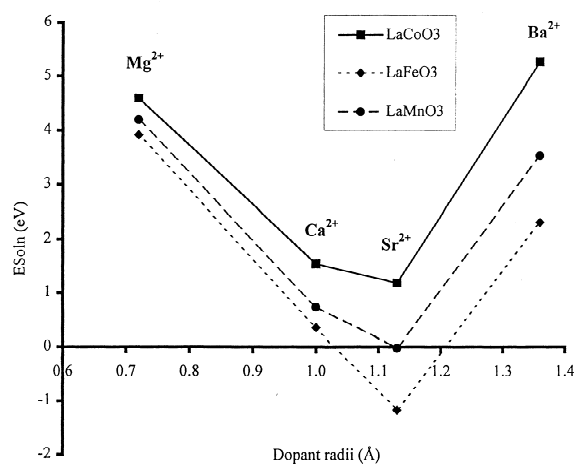


Fig. 1. Energies of solution as a function of ion size for alkaline-earth dopants in  $\text{LaMO}_3$ .

vacancies. This accords well with experimental work in which these ions are the most commonly used acceptor dopants in  $\text{LaMO}_3$  to generate high proton (and oxygen ion) conductivity [17–19].

Protons are introduced into these materials by treatment in water vapour, whereby oxygen vacancies are filled by hydroxyl ions; the defect is described as a hydroxyl group as the interstitial proton is closely associated with the neighbouring oxygen ion. The water incorporation reaction can be described as follows:



In this way protons replace oxygen ion vacancies as charge-compensators for the acceptor dopants. The energy for the incorporation of water into the doped material ( $E_{\text{react}}$ ) can be evaluated using the following equation:

$$E_{\text{react}} = 2E_{\text{OH}} - E(\text{V}_{\text{O}}^{\bullet\bullet}) + E_{\text{PT}} \quad (3)$$

where  $E_{\text{OH}}$  is the energy associated with substitution by the hydroxyl group,  $E(\text{V}_{\text{O}}^{\bullet\bullet})$  the energy of an oxygen vacancy, and  $E_{\text{PT}}$  the energy of the gas phase proton transfer reaction:  $\text{O}^{2-} + \text{H}_2\text{O} \rightarrow 2\text{OH}^{\cdot}$ . Using these terms, the energy of incorporation of water ( $E_{\text{react}}$ ) into  $\text{LaMnO}_3$  is calculated to be  $-0.88$  eV and hence exothermic; this suggests that the dissolution of protons at the expense of oxygen vacancies is favoured by decreasing temperatures in this oxide. Although corresponding experimental data is limited, our results are consistent with the measured negative enthalpies for this reaction in  $\text{LaErO}_3$  [18] and in rare-earth oxides ( $\text{Y}_2\text{O}_3$ ,  $\text{Sm}_2\text{O}_3$ ,  $\text{Gd}_2\text{O}_3$ ) [26].

### 3.2. Proton transfer and lattice relaxation

Isotope effect ( $\text{D}^+$  vs  $\text{H}^+$ ) measurements of perovskite oxides [20] have suggested that the conduction mechanism is due to proton hopping between adjacent oxygen ions (Grotthuss-type mechanism), rather than by hydroxyl ion migration ('vehicle' mechanism). These studies also imply that the proton jump is non-classical but involves quantum mechanical terms. We have therefore used ab initio Hartree–Fock techniques to investigate the proton

transfer process, and specifically to derive the energy barrier to the process  $\text{OH}^{\cdot} \dots \text{O}^{2-} \rightarrow \text{O}^{2-} \dots \text{HO}^{\cdot}$ .

It has been suggested that proton transfer rather than hydroxyl ion reorientation is the rate-limiting step for proton conductivity in metal oxides [2,21]. In this study, we have evaluated the energy barrier to proton transfer by a simple hopping mechanism as the difference in energy between two states: (i) the ground state in which the single hydrogen is effectively bound to an oxygen ion, and (ii) the barrier state in which the hydrogen is equidistant between both the adjacent oxygen ions, which is illustrated in Fig. 2. The calculated barrier energy as a function of O–O separation is presented in Table 1. All energies after inclusion of correlation are small; the lowest of  $\sim 0.02$  eV is only of the order of the zero point energy of the free OH-species, although the magnitude increases slightly with increasing O–O separation.

With regard to the ground state configuration, the predicted O–H geometry has the proton site near the direction of one neighbouring oxygen ion with an equilibrium O–H bond distance of  $0.94$  Å. The relaxed geometry of the barrier state configuration shows the importance of the O–O separation in the transfer process, as proposed by Kreuer et al. [21]. Table 2 presents the initial (unrelaxed) and final

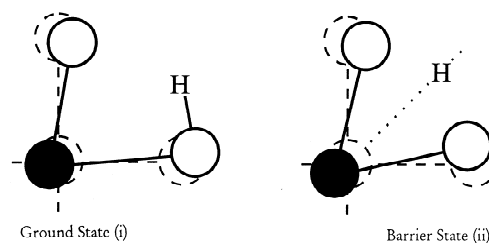


Fig. 2. Ground and barrier state configurations for proton transfer between neighbouring oxygen ions. (Dashed and full lines indicate perfect lattice and relaxed geometries respectively.)

Table 1  
Variation in the energy barrier ( $E_b$ ) with initial O...O separation

Initial O...O separation (Å)	Energy (eV)
2.67	0.02
2.76	0.04
2.90	0.16

Table 2

Initial and final O...O separations for the barrier state configuration in the proton transfer process

Initial (unrelaxed) separation (Å)	Final (relaxed) separation (Å)
2.67	2.32
2.76	2.35
2.90	2.38

(relaxed) O–O separations from the barrier state calculations, which indicate that in each case the separation reduces to a value below ca. 2.4 Å so as to assist proton transfer. This result corresponds to a significant hydrogen bond interaction which contracts the O–O distance so the proton is not transferred through a completely isolated state.

Our calculated energy barriers are well below the observed activation energies of 0.4–0.7 eV for the total proton conductivity process in LaMO<sub>3</sub> perovskite-type oxides [17,18]. This difference suggests that the activation energy for proton migration may depend on other energy terms. For the proton transfer process our ab initio cluster calculations yield the energy and geometry of the ground and barrier state configurations. However, they provide no information concerning the relaxation of the surrounding lattice which would accompany the proton migration. Moreover, if protons migrate by a ‘barrier-less’ jump or by a tunnelling process it will be essential that lattice relaxation achieves an equivalent environment around the two oxygen sites before transfer can occur i.e., states of identical energy should be available on both sides of the barrier. Migration would thus occur via the process shown schematically in Fig. 3.

We propose that the energy required to obtain this intermediate state, which precedes the proton transfer, is the major constituent of the activation energy

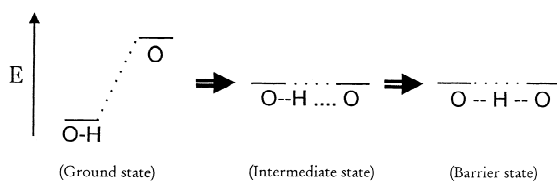


Fig. 3. Schematic representation of the proton transfer process indicating equilibration of the energy levels of the two adjacent oxygen ions.

Table 3

Energy terms associated with the lattice relaxation needed to generate equivalent environments about two adjacent oxide ions in LaMnO<sub>3</sub>

Energy state	Energy (eV)
$E_{\text{OH}}$	7.34
$E_{\text{int}}$	8.03
$E_{\text{relax}}$	0.69

for proton conductivity. Atomistic simulations have been performed to evaluate this ‘equivalencing’ energy, i.e., the energy required to move from the initial ground state with the proton bound to one oxygen ion to the intermediate state where the oxygen ions are in equivalent environments and separated by less than 2.4 Å. The energy of the ground state configuration is simply  $E_{\text{OH}}$ , the energy of substituting an oxide ion with a hydroxyl group. We have obtained a value for the intermediate state using the energy-minimised positions of the lattice ions when the proton and adjacent oxygen ions are in the barrier state configuration.

The relaxation energy ( $E_{\text{relax}}$ ) for proton migration is calculated as the difference in energy between the intermediate state ( $E_{\text{int}}$ ) as described above and the ground state ( $E_{\text{OH}}$ ). The results for this series of calculations and the value of  $E_{\text{relax}}$  are given in Table 3. It is significant that we find a value of 0.69 eV for  $E_{\text{relax}}$  which correlates with observed activation energies for proton conductivity in perovskite oxides. Although experimental data for LaMnO<sub>3</sub> is unavailable, this value is consistent with measured activation energies of 0.7 eV for doped LaYO<sub>3</sub> [17] and 0.42–0.50 eV for doped LaErO<sub>3</sub> [18]. The calculations therefore suggest that a key step before proton transfer is the energy required for the neighbouring oxide ions to acquire equivalent lattice environments. This relaxation effect may be favoured in structures with only one type of crystallographic oxygen site by avoiding extra terms associated with energy differences between non-equivalent positions.

#### 4. Summary

The work discussed in this paper demonstrates that the complementary use of atomistic simulation and ab initio techniques can assist in providing a deeper

understanding of proton transport phenomena in perovskite-structured oxides.

Three main points emerge from our results. First, incorporating water into  $\text{LaMnO}_3$  is found to be exothermic, indicating that the dissolution of protons at the expense of oxygen vacancies is favoured by decreasing temperatures, in accord with the available thermodynamic data. Sr and Ca dopants will enhance proton uptake by increasing the oxygen vacancy concentration owing to their low solution energies. Second, the *ab initio* cluster calculations find a very low energy barrier to proton transfer between neighbouring oxygen ions. The relaxed geometry of the barrier state shows a contraction of the O-O separation so as to assist proton transfer. Finally, a critical step for proton migration, we believe, is the relaxation energy required for the neighbouring oxygen ions to acquire equivalent lattice environments (or energy states) before proton transfer.

### Acknowledgments

We thank J.D. Gale and C.R.A. Catlow for valuable discussions. This work was supported by the EPSRC and BP Research.

### References

- [1] H. Iwahara, *Solid State Ionics* 77 (1995) 289.
- [2] K.D. Kreuer, *Chem. Mater.* 8 (1996) 610.
- [3] H. Iwahara, T. Esaka, H. Uchida, N. Maeda, *Solid State Ionics* 3/4 (1981) 359.
- [4] T. Yajima, H. Iwahara, *Solid State Ionics* 50 (1992) 281.
- [5] T. Yajima, H. Iwahara, *Solid State Ionics* 53–56 (1992) 983.
- [6] K.D. Kreuer, E. Schönher, J. Maier, *Solid State Ionics* 70–71 (1994) 278.
- [7] J.F. Liu, A.S. Nowick, *Solid State Ionics* 50 (1992) 131.
- [8] N. Bonanos, K.S. Knight, B. Ellis, *Solid State Ionics* 79 (1995) 161.
- [9] R.C.T. Slade, S.D. Flint, N. Singh, *J. Mater. Chem.* 4 (1995) 509.
- [10] Th. Matzke, U. Stimming, Ch. Karmonik, M. Soetratmo, R. Hemplemann, F. Güthoff, *Solid State Ionics* 86–88 (1996) 621.
- [11] R.A. De Souza, J.A. Kilner, B.C.H. Steele, *Solid State Ionics* 77 (1995) 180.
- [12] T. Yajima, H. Kazeoka, T. Yogo, H. Iwahara, *Solid State Ionics* 47 (1991) 271.
- [13] J.A. Labrincha, J.R. Frade, F.M.B. Marques, *Solid State Ionics* 61 (1993) 71.
- [14] L. Zimmermann, H.G. Bohn, W. Schilling, E. Syskakis, *Solid State Ionics* 77 (1995) 163.
- [15] T. Schober, J. Friedrich, J.B. Condon, *Solid State Ionics* 77 (1995) 175.
- [16] H. Yugami, S. Matsuo, M. Ishigame, *Solid State Ionics* 77 (1995) 195.
- [17] E. Ruiz-Trejo and J.A. Kilner, *Solid State Ionics* 97 (1997) 529 (this issue).
- [18] Y. Larring, T. Norby, *Solid State Ionics* 70/71 (1994) 305.
- [19] B.C.H. Steele, in: M. Balkanski, T. Takahashi and H.L. Tuller, Eds., *Solid State Ionics*, Elsevier, Amsterdam, 1992.
- [20] K.C. Liang, Y. Du, A.S. Nowick, *Solid State Ionics* 69 (1994) 117.
- [21] K.D. Kreuer, A. Fuchs, J. Maier, *Solid State Ionics* 77 (1995) 157.
- [22] M. Cherry, M.S. Islam, C.R.A. Catlow, *J. Solid State Chem.* 118 (1995) 125.
- [23] M.S. Islam, M. Cherry, C.R.A. Catlow, *J. Solid State Chem.* 124 (1996) 230.
- [24] C.R.A. Catlow, in: A.K. Cheetham and P. Day, Eds., *Solid State Chemistry: Techniques*, Clarendon, Oxford, 1987.
- [25] R.D. Amos, *CADPAC v5.1*, Cambridge University, 1992.
- [26] T. Norby, O. Dyrlye, P. Kofstad, *J. Am. Ceram. Soc.* 75 (1992) 1176.